Mechanism of Trapping Effect in Heterojunction With Intrinsic Thin-Layer Solar Cells: Effect of Density of Defect States

X. Hua, Z. P. Li, W. Z. Shen, G. Y. Xiong, X. S. Wang, and L. J. Zhang

***Abstract*—We have simulated the performance of heterojunction with intrinsic thin-layer (HIT) solar cells on n-type c-Si substrates using the numerical simulator automat for simulation of heterostructures (AFORS-HET), with emphasis on the effect of density of defect states (DOS) in both p-type hydrogenated amorphous silicon (a-Si:H) emitter and intrinsic a-Si:H buffer layers. A detailed and accurate DOS distribution, including both bandtail states and deep dangling-bond states, has been established in a-Si:H layers based on existing experimental results of a-Si:H films in the literature. The changes of DOS distribution for differently doped thin a-Si:H layers, depending on their doping concentrations (from intrinsic to highly doped), have explicitly been considered. With this DOS distribution model, we have calculated the charge trapped in defect states, which understands the mechanism of trapping effect, i.e., how the DOS influences the built-in field, space-charge region, and the cell performance within HIT solar cell structures. It is found that the DOS in the p-type a-Si:H emitter layer can cause an unfavorable trapping effect, which becomes more serious and even difficult to avoid in case of high doping concentration beyond 1×10^{20} cm^{-3}. In contrast, the DOS in the intrinsic a-Si:H buffer layer will not sufficiently suppress the cell output until the density of dangling-bond states reaches 5×10^{18} cm^{-3}. This paper presents a clear physical picture for the mechanism of trapping effect and concludes the suggestive DOS required for the high efficiency of HIT cells above 20%.**

***Index Terms*—Amorphous semiconductors, doping, photovoltaic cells, semiconductor device modeling, semiconductor impurities, solar energy.**

I. Introduction

HETEROJUNCTION with intrinsic thin-layer (HIT) solar cells combine the high stable efficiency of crystalline silicon (c-Si) with the low-temperature deposition technology of hydrogenated amorphous silicon (a-Si:H) films, leading to a sufficient cut of production cost of high-efficiency solar cells. HIT solar cells have attracted much more attention as a possible low-cost alternative to c-Si solar cells, which creates a great prospect of the photovoltaic market. Sanyo Electric Co. Ltd., Osaka, Japan, has promoted the record of conversion efficiency to 23.0% in 2011 [1] for a practical size of 100.4 cm^2 in HIT structures on n-type c-Si substrates and will soon report their new improvement to 23.7% in 98-μm-thin wafers. Several European and U.S. groups have also achieved the conversion efficiency around 20%, both on n- and p-type c-Si substrates [2]–[4].

To understand the key issues of HIT high efficiency, recent studies have focused on the carrier transport mechanisms [5]–[7] and the optimization of structures [8]–[11]. Computer modeling has widely been carried out to evaluate the role of various controlling factors of the HIT structure. Froitzheim *et al.* [12] and Datta *et al.* [11], [13] have established the strong influence of the defect states at a-Si:H/c-Si interfaces. Combining their experimental data with modeling results, they raise the importance of the heterointerface treatment and passivation of defects on the surface of c-Si wafer, which matches well with many other groups [5], [9], [10]. Kanevce *et al.* [6] have examined the role of transparent conductive oxide (TCO) by modeling the TCO as an n-type semiconductor layer, essentially forming an n–p–n structure. Some other groups have shown the effect of thickness and doping concentration of the individual layers and drawn the conclusion that the a-Si:H layer should be ultrathin and extremely heavily doped to achieve the high efficiency above 20% [8], [9].

It is well known that there must be a large density of defect states (DOS) and even significant trapping effect in ultrathin and/or heavily doped a-Si:H films, which will greatly reduce the cell performance. Nevertheless, few studies have taken into account the effect of the DOS in a-Si:H films. The difficulty lies in the fact that a detailed and accurate DOS distribution is needed, which has been simplified by some researchers [9]. Note that the accuracy of the model can be critical, because the result is quite sensitive upon the parameters utilized in the simulation. In this paper, we have employed the numerical computer simulator automat for simulation of heterostructures (AFORS-HET) to simulate Sanyo's new structure of HIT solar cells, focusing on the effect of DOS in both p-type a-Si:H emitter and intrinsic a-Si:H buffer layers upon cell performance. We have established a more accurate

Manuscript received October 24, 2011; revised December 15, 2011 and January 21, 2012; accepted January 23, 2012. Date of publication February 13, 2012; date of current version April 25, 2012. This work was supported in part by the National Major Basic Research Program of China through Projects 2011AA050502 and 2012CB934302 and the Natural Science Foundation of China under Contracts 11074169 and 11174202. The review of this paper was arranged by Editor A. G. Aberle.

X. Hua, Z. P. Li, and W. Z. Shen are with the Laboratory of Condensed Matter Spectroscopy and Optoelectronic Physics, the Key Laboratory of Artificial Structures and Quantum Control (Ministry of Education), and the Institute of Solar Energy, Department of Physics, Shanghai Jiao Tong University, Shanghai 200240, China (e-mail: wzshen@sjtu.edu.cn).

G. Y. Xiong, X. S. Wang, and L. J. Zhang are with the R&D Center, Canadian Solar Inc., Suzhou 215129, China.

Color versions of one or more of the figures in this paper are available online at http://ieeexplore.ieee.org.

Digital Object Identifier 10.1109/TED.2012.2186139

0018-9383/$31.00 © 2012 IEEE

TABLE I
PARAMETERS USED FOR THE SIMULATION

Parameters	*a*-Si:H (p)	*a*-Si:H (i)	Front interface	c-Si (n)	Rare interfaces	*a*-Si:H (n^+)
Layer thickness (cm)	6.5×10^{-7}	3.0×10^{-7}		3.0×10^{-2}		5.0×10^{-7}
Mobility gap E_g(eV)	1.75	1.75		1.12		1.80
Optical gap (eV)	1.74	1.74		1.12		1.78
Donor (accepter) doping (cm^{-3})	(7.5×10^{19})	0		1.5×10^{16}		7.0×10^{19}
Dielectric constant ε	11.9	11.9		11.9		11.9
Electronic affinity (eV)	3.90	3.90		4.05		3.90
Effective band density (cm^{-3})	1.0×10^{20}	1.0×10^{20}		2.8×10^{19}		1.0×10^{20}
Electron (hole) mobility (cm^2/Vs)	25 (5)	25 (5)		1111 (421.6)		20 (5)
Richardson constant for electron (hole) (As/cm^2sK^2)			110.0 (147.5)		110.0 (147.5)	
Bandtail states						
Defect density at conduction band edge (cm^{-3}/eV)	2×10^{21}	2×10^{21}				4×10^{21}
Defect density at valence band edge (cm^{-3}/eV)	2×10^{21}	2×10^{21}				2×10^{21}
Urbach energy for conduction bandtail (eV)	0.037	0.020				0.037
Urbach energy for valence bandtail (eV)	0.045	0.045				0.081
Neutral (charged) σ (cm^{-2})	7×10^{-17} (7×10^{-16})	1×10^{-14} (1×10^{-12})				7×10^{-17} (7×10^{-16})
Dangling-bond states						
Maximum defect density (cm^{-3}/eV)	2.0×10^{18} -1.4×10^{20}	1.0×10^{17} -1.0×10^{20}				1.4×10^{20}
Maximum defect density in interface (cm^{-2}/eV)			2.4×10^{11}		2.4×10^{11}	
Peak position beyond E_V for $D^{0/+}$($D^{-/0}$) (eV)	1.10 (1.35)	0.725 (1.025)	1.10		1.10	0.40 (0.65)
FWHM (eV)	0.4	0.2	0.4		0.4	0.4
Neutral (charged) σ (cm^{-2})	3×10^{-14} (3×10^{-13})	1×10^{-14} (1×10^{-12})	(1×10^{-17})		(1×10^{-17})	3×10^{-14} (3×10^{-13})
Total defect density (cm^{-3})	1.0×10^{18} -7.0×10^{19}	2.5×10^{16} -2.5×10^{19}				7.0×10^{19}
Total defect density in interface (cm^{-2})			1.2×10^{11}		1.2×10^{11}	

DOS distribution in *a*-Si:H through the experimental results of *a*-Si:H bulk and surface [2], [14]–[17] and used it to understand the mechanism of trapping effect, i.e., how the DOS affects the built-in field and space-charge region (SCR), as well as cell output. We have demonstrated the proper DOS required in *a*-Si:H layers to achieve efficiency above 20% of HIT solar cells under various doping concentrations in practical production.

II. NUMERICAL MODEL FOR HIT SIMULATION

AFORS-HET, the numerical computer simulator designed for heterojunction devices and later extended to HIT cells [2], [8], [18], is utilized for solving 1-D Poisson and continuity semiconductor equations in this paper. The simulated HIT cell structure on the n-type c-Si substrate is TCO/p-*a*-Si:H/i-*a*-Si:H/n-c-Si/ n^+-*a*-Si:H(BSF)/Al, referred to as Sanyo's HIT structure. Note that, although we ignore the i-*a*-Si:H layer of the rare side for the lack of precise experimental data, we still include a well-passivated interface on the rare surface of c-Si wafer with low interface defect density. The values of the parameters adopted for simulation are listed in Table I.

In the simulation of optical properties, the incident light (standard air mass of 1.5 illumination spectrum, i.e., AM 1.5) enters through the TCO/p-*a*-Si:H emitter layer. We take proper

account of light reflection and absorption in the TCO film and introduce textured pyramid structure on the front surface of the c-Si wafer. We calculate the multiple reflection and coherence, depending on the incident light wavelength of each a-Si:H layer and c-Si substrate. However, optical impacts such as the light-trapping effect and grid shading are not involved like other modelers [5]–[8], [11], [18].

The simulation of electrical properties is constructed with the following three parts: 1) contacts; 2) interfaces; and 3) bulk layers. The junction between TCO and the p-type a-Si:H layer is taken as $x = 0$ on the position scale and referred to as the front contact, where the work function of the standard TCO is fixed at 5.2 eV. On the other hand, to focus on the effect in the emitter and buffer layers, we assume a conventional Al contact and flatband condition at the back contact, instead of TCO used in Sanyo's 2011 HIT structure to remove the complex influence of back-contact barrier, because the TCO of rare side still needs further investigation for more experimental results. Both surface recombination velocities of electrons and holes at the front and back contacts are set as 1×10^7 cm/s.

Defect states at both front and rear a-Si:H/c-Si interfaces are assumed to be Gaussian distributed, with peaks located at the midgap of c-Si, based on the experimental results in the a-Si:H near-surface layers by Winer *et al.* [16]. The total DOS at interfaces is set as a low value of 1.2×10^{11} cm^{-3}, which does not result in a modified band bending [12]. Carrier transport across the a-Si:H/c-Si interface is modeled through thermionic emission, and the tunneling process is not included, because the current of tunneling is unlikely to affect solar cell performance at its normal working condition [13].

In bulk layers, semiconductor equations are solved using the Shockley–Read–Hall (SRH) recombination model [19] for steady-state conditions under external illumination. Band diagrams and band offsets are calculated according to the Anderson model and matches well with the experimental measurements at the a-Si/c-Si heterojunction [20], [21]. The defect states in the c-Si substrate are assumed to be uniformly distributed and acceptor-like for the main O-vacancy defects in c-Si [22], whereas in the a-Si:H emitter and buffer layers, the DOS distribution is more complicated and can strongly influence the recombination in bulk layers, which may further impact the cell output. The details of DOS distribution in a-Si:H is modeled in Section III.

III. DOS Distribution Model for a-Si:H

As the key issue to understand the effect of the DOS in a-Si:H emitter and buffer layer upon HIT cell performance, an elaborate DOS distribution model based on existing experimental results is established, which takes the measured DOS distributions for differently doped thin a-Si:H film into account. The defect states in a-Si:H mainly consist of exponential bandtail states and deep dangling-bond (DB) states. As shown in Fig. 1(a)–(c), the conduction and valence bandtail states are accepter- and donor-like, respectively, and both have exponential distribution in energy E. The total defect density of conduction bandtail (C bandtail) states (N_{Ctail}) and valence bandtail (V bandtail) states (N_{Vtail}) are usually given as follows:

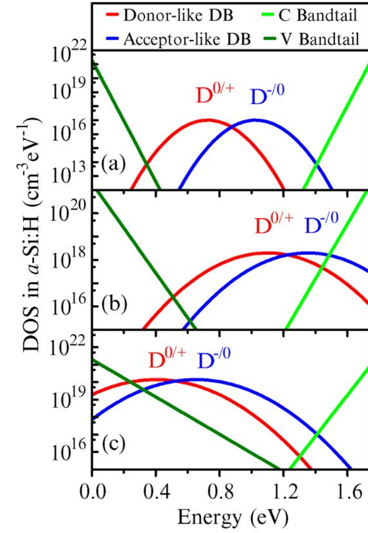

Fig. 1. DOS distribution model, including donor-like DB, acceptor-like DB, C bandtail, and V bandtail states. DOS distribution in (a) intrinsic a-Si:H buffer layer and (b) p-type a-Si:H emitter layer (with an effective doping level, i.e., difference of the Fermi level to the valence band edge, $E_F - E_V = 45$ meV, which is quite small because of the heavily doped and low DOS condition), and (c) heavily doped n-type a-Si:H BSF (with effective doping level $E_C - E_F = 220$ meV).

$$N_{\text{Ctail}}(E) = \int_{E_V}^{E_C} N_{\text{OC}} \exp\left(\frac{E - E_C}{E_{\text{OC}}}\right) dE$$

$$N_{\text{Vtail}}(E) = \int_{E_V}^{E_C} N_{\text{OV}} \exp\left(\frac{E_V - E}{E_{\text{OV}}}\right) dE \quad (1)$$

where N_{OC} and N_{OV} denote the densities per energy range at the conduction (E_C) and valence (E_V) band edges, respectively. They are used here to define a quantitative scale for DOS distribution. E_{OC} and E_{OV} are the Urbach energies, i.e., the inverse logarithmic slope of the conduction and valence bands, reflecting the disorder broadening of bands.

The values of N_{OC} and N_{OV} amount to 2×10^{21}–4×10^{21} cm^{-3}/eV and hardly vary with doping concentration, yielded from various measurements by many researchers [16], [17], [23], [24]. Schmidt *et al.* [2] have employed a fixed number of 2×10^{21} cm^{-3}/eV for N_{OV} to normalize their constant final state yield spectroscopy results on ultrathin a-Si:H films. The Urbach energies E_{OC} and E_{OV}, which characterize the shape of bandtail states, show different sensitivities to doping condition. The value of E_{OV} preserves between 43 and 51 meV, keeping almost unchanged in both intrinsic and boron-doped a-Si:H films [16], whereas E_{OV} can increase to 61 meV in phosphorus-doped a-Si:H [15], and even higher than 101 meV for ultrathin films (~2.8 nm) [14]. However, E_{OC} is 34–37 meV in phosphorus-doped a-Si:H and appears a little sensitive to doping condition [16]. Both E_{OC} and E_{OV} rise for thinner and more defective a-Si:H films because of the increment of disorder.

The more important defects are deep DB states as they lie near the midgap to be effective recombination centers, and they are very sensitive to various production conditions. This family of deep defects (D) can be pictured as dangling sp-hybrid orbitals of Si atoms in different nearest neighbor environments. D^0 is its neutral state, where a DB orbital is occupied by a single valence electron of the corresponding Si atom. The DB states that correspond to the D^0/D^+ $(D^+ + e^- \rightarrow D^0)$ and D^-/D^0 $(D^0 + e^- \rightarrow D^-)$ transitions can be characterized by deep-level transient spectroscopy (DLTS) and electron-spin-resonance (ESR) measurements [25]–[27]. The total density of states within the mobility gap can also be yielded using ultraviolet-excited photoelectron-yield spectroscopy, photothermal deflection spectroscopy, and total-yield methods [14], [16], [17], [25]. It is found that the DB states are continuously distributed, fitted as two Gaussian distribution functions [25] that correspond to the D^0/D^+ and D^-/D^0 transitions [see Fig. 1(a)–(c)]. The density of donor-like (N_{tD}) and acceptor-like (N_{tA}) DB states are given as

$$N_{\mathrm{tD}} = \int_{E_V}^{E_C} N_{D0} \exp\left[-\frac{(E - E^{0/+})^2}{2(\mathrm{FWHM}/2)^2}\right] dE$$

$$N_{\mathrm{tA}} = \int_{E_V}^{E_C} N_{A0} \exp\left[-\frac{(E - E^{-/0})^2}{2(\mathrm{FWHM}/2)^2}\right] dE \qquad (2)$$

where N_{D0} and N_{A0} are the peak values of defect states that correspond to the D^0/D^+ and D^-/D^0 transitions, respectively, with $E^{0/+}$ and $E^{-/0}$ being the peak energy positions beyond E_V and FWHM the full width at half maximum of the Gaussian profile.

We assume the defect states distribution in the a-Si:H bulk to be symmetric and set the density of DB states $N_t = N_{\mathrm{tA}} = N_{\mathrm{tD}}$ for convenience. Note that, because the asymmetry distribution is very common in amorphous materials, further study of broken symmetry condition will be discussed in Section IV. N_{D0} and N_{A0} vary with the doping concentration, from $\sim 1 \times 10^{16}$–2×10^{19} cm^{-3}/eV in intrinsic films [16], [17] to higher than 1×10^{20} cm^{-3}/eV in highly doped a-Si:H [10], which shall further increase for thinner films, particularly for the ultrathin films used as HIT emitter and buffer layers. The value of FWHM has been derived to be 0.2 eV in intrinsic a-Si:H films based on the experimental results in [17] and is found to be 0.4 eV in doped a-Si:H in [16] based on the total yield measurements.

The peak positions of Gaussian profile $E^{0/+}$ and $E^{-/0}$ greatly affect N_t when their positions come very close to the band edge and sensitively work on the charge trapped in defect states [see (5) in Section IV]. However, the changes of peak position have easily been ignored by other groups [9]. In intrinsic a-Si:H films, $E^{0/+}$ and $E^{-/0}$ lie near the midgap at $E_V + 0.725$ and $E_V + 1.025$ eV, respectively [17]. Winer *et al.* [16] have observed that, in highly doped n-type a-Si:H, the shift of $E^{0/+}$ and $E^{-/0}$ toward E_V (relative to their positions in intrinsic a-Si:H) is equal to the shift of Fermi level E_F in the opposite direction. Similarly, in p-type a-Si:H, we can also assume that the shift of $E^{0/+}$ and $E^{-/0}$ toward E_C is equal to the shift of E_F toward E_V.

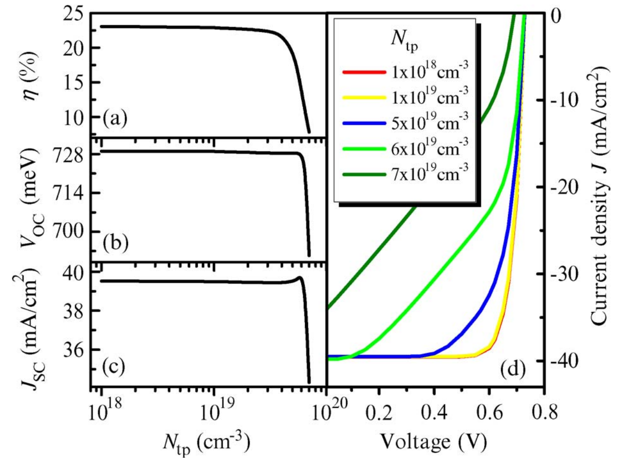

Fig. 2. Effect of the density of DB states (N_{tp}) in the p-type a-Si:H emitter layer on the HIT cell performance of (a) efficiency (η), (b) open-circuit voltage (V_{OC}), (c) short-circuit current density (J_{SC}), and (d) J–V curves under illumination.

The distribution of donor- and acceptor-like states is determined by the effective correction energy U_{eff} $(D^0 + D^0 + U_{\mathrm{eff}} \rightarrow D^+ + D^-)$ between singly and doubly occupied D^0 defects. When $U_{\mathrm{eff}} > 0$, the lower midgap defect states (D^0/D^+) are donor-like, and the upper midgap defect states (D^-/D^0) are acceptor-like. It is convincingly concluded through DLTS and ESR measurements that U_{eff} is positive, in the range of 0.2–0.4 eV [27]. In combination with other observations of roughly 0.3 eV [28], we attribute that the D^0/D^+ transition lies 0.25–0.30 eV (depending on doping concentration) below the D^-/D^0 transition.

IV. Effect of Increasing the Amount of Defects in p-Type Emitter Layers

Fig. 2(a)–(c) illustrates the dependence of the density of DB states (N_{tp}) in the p-type a-Si:H emitter layer (with a doping concentration of $N_A = 7.5 \times 10^{19}$ cm^{-3}) on HIT cell performance. We vary N_{tp} in the range of 1×10^{18}–7×10^{19} cm^{-3}, with a relatively low density of DB states in the intrinsic buffer layer fixed at 2.5×10^{16} cm^{-3}. As shown in Fig. 2(a)–(c), the cell conversion efficiency (η) and open-circuit voltage (V_{OC}), as well as short-circuit current density (J_{SC}), keep almost unchanged at N_{tp} below 1×10^{19} cm^{-3}, where the yielded η of 23.0%, V_{OC} of 729 mV and J_{SC} of 39.52 mA/cm^2 are in excellent agreement with Sanyo's 2011 records [1]. With N_{tp} increasing to 5×10^{19} cm^{-3}, a slow decrease of the HIT cell performance can be observed. In contrast, the parameters of the cell performance exhibit a sharp fall when N_{tp} approaches the doping concentration of the emitter layer. The abnormal increment of J_{SC} at 6×10^{19} cm^{-3} will be explained later by the carrier recombination and collection.

In Fig. 2(d), we have also shown the effect of N_{tp} on the current density–voltage (J–V) curve of the HIT cell. The shape of the J–V curve characterizes the filled factor (FF) and stays almost the same under low $N_{\mathrm{tp}} < 5 \times 10^{19}$ cm^{-3}. When N_{tp}

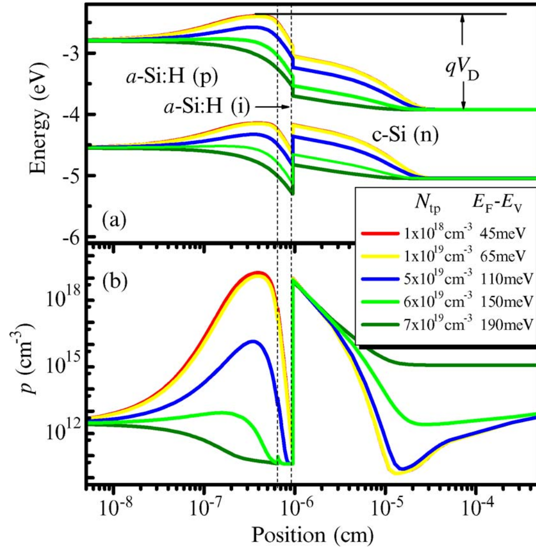

Fig. 3. (a) Band diagram and (b) free-hole concentration (p) under different densities of DB states $(N_{\rm tp})$ in the p-type a-Si:H emitter layer calculated under the open-circuit condition. $E_F - E_V$ is the difference of the Fermi level to the valence band edge, corresponding to different $N_{\rm tp}$.

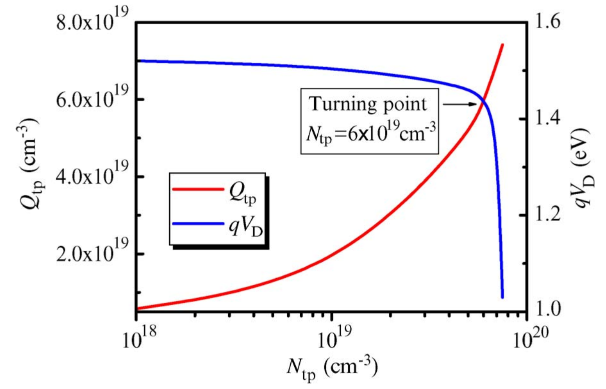

Fig. 4. Calculated charge trapped in defect states of the p-type a-Si:H emitter layer $(Q_{\rm tp})$ and the difference of potential energy (qV_D) between the p-type a-Si:H layer and the n-type c-Si side as a function of the density of DB states $(N_{\rm tp})$ in the emitter layer under the open-circuit condition.

arises to the high level of 6×10^{19} cm^{-3}, it turns out that FF has significantly reduced, resulting in the great decay of cell performance. In conclusion, the proper $N_{\rm tp}$ required for high efficiency above 20% should be suppressed below 6×10^{19} cm^{-3} to avoid trapping effect, whereas the improvement appears inconspicuous for further decrease of $N_{\rm tp}$ to lower than 1×10^{19} cm^{-3}.

In Fig. 3(a), we display the band diagram of the HIT cell under standard AM 1.5 (open circuit) to understand the effect of the DOS in the p-type a-Si:H emitter layer (the interfaces are marked with dotted lines). It is found that the band diagram varies little at $N_{\rm tp}$ below 1×10^{19} cm^{-3}. However, when $N_{\rm tp}$ rises to 5×10^{19} cm^{-3}, the a-Si:H side becomes more depleted, whereas the depletion region of the c-Si side shrinks. The depletion region of the c-Si side almost vanishes at the high $N_{\rm tp}$ of 7×10^{19} cm^{-3}, with a significant decay of the barrier height V_D in the conduction band between the p-type a-Si:H layer and the n-type c-Si wafer, resulting in the pile-up of holes at a-Si:H/c-Si interface in Fig. 3(b).

This observation indicates that the high DOS in the a-Si:H layer leads to a shift of SCR from c-Si to a-Si:H and a reduction of the built-in field. We introduce the charge trapped in defect states Q_t to quantitatively study how the density of DB states N_t works on the built-in field, SCR, and further cell output. Taking Q_t into account, the Poisson equation in SCR should be modified as

$$\frac{\partial^2 V(x)}{\partial x^2} = \frac{q}{\varepsilon}\left[-N_A(x) + N_D(x) + p(x) - n(x) + Q_t(x)\right] \tag{3}$$

where V denotes the potential, x is the position, q is the electron charge, and ε is the dielectric constant. N_A and N_D are the concentrations of doping acceptors and donors (assumed to be completely ionized), respectively. n and p are the non-equilibrium electron and hole concentrations that satisfy the Boltzmann statistics, i.e.,

$$\begin{cases} n = N_C \exp\left(-\frac{E_C - E_F^n}{KT}\right) \\ p = N_V \exp\left(-\frac{E_F^p - E_V}{KT}\right) \end{cases} \tag{4}$$

where N_C is the effective conduction band density, N_V is the effective valence band density, K is the Boltzmann constant, and T is the temperature. E_F^n and E_F^p are the quasi-Fermi energies of electrons and holes, Q_t is integrated, referred to as the SRH recombination model, i.e.,

$$\begin{cases} Q_t = -\int_{E_V}^{E_C} dE f_t(E) N_{\rm tA}(E) + \int_{E_V}^{E_C} dE\,(1 - f_t(E))\, N_{\rm tD}(E) \\ f_t(E) = \frac{n + N_V \exp\left(-\frac{E-E_V}{KT}\right)}{p + n + N_C \exp\left(-\frac{E_C - E}{KT}\right) + N_V \exp\left(-\frac{E-E_V}{KT}\right)} \end{cases} \tag{5}$$

where $f_t(E)$ is a distribution function that specifies the probability that defects with a density of $N_t(E)$ at the position E within the bandgap are occupied with electrons.

We extract $Q_t(x)$ (i.e., Q_t depends on the position x) from AFORS-HET and integrate it to calculate the trapped charge in the p-type layer $Q_{\rm tp}$ (under the open-circuit condition), which is presented in Fig. 4. Based on (3), we can simplify the effective doping concentration and charge density in the p-type SCR as $(N_A - Q_{\rm tp})$ for convenience, because n and p can be neglected because they are relatively low under the heavily doping condition of $N_A = 7.5 \times 10^{19}$ cm^{-3}. It is found that, in Fig. 4, $Q_{\rm tp}$ remains below 1.5×10^{19} cm^{-3} for $N_{\rm tp} < 1 \times 10^{19}$ cm^{-3}, indicating a small difference between $(N_A - Q_{\rm tp})$ (beyond 6×10^{19} cm^{-3}) and N_A. On the other hand, $Q_{\rm tp}$ reaches a fairly high value of 6.93×10^{19} cm^{-3} in the case of $N_{\rm tp} = 7 \times 10^{19}$ cm^{-3}, whereas $(N_A - Q_{\rm tp})$ decreases to 1.7×10^{18} cm^{-3}, an order of magnitude lower than N_A, resulting in a significant trapping effect. Consequently, $Q_{\rm tp}$ strongly influences effective doping concentration and the charge density in the p-type SCR, particularly when it becomes comparable to N_A, leading to the observed decreased V_D and a shift of SCR from the c-Si to the a-Si:H side, as demonstrated in Fig. 3(a).

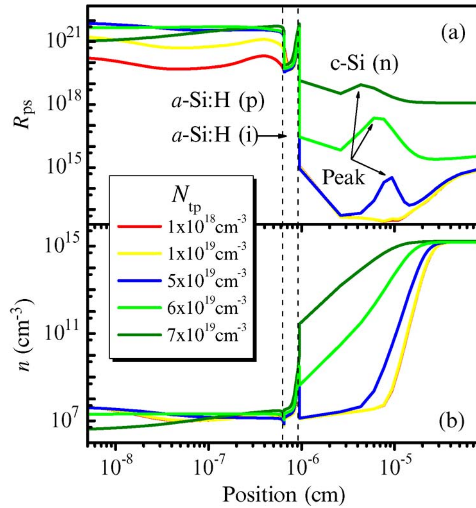

Fig. 5. (a) Hole recombination rate (R_p) and (b) free-electron concentration (n) under conditions of different densities of DB states $(N_{\rm tp})$ in the emitter layer under the open-circuit condition.

We first extracted the value of qV_D [see Fig. 4] from AFORS-HET calculating results to see the effect on the HIT cell performance. V_D denotes the barrier height for electrons that move from n-c-Si to p-a-Si:H in the conduction band, which helps us understand the change of built-in field. It is found that qV_D sufficiently varies only when $N_{\rm tp}$ reaches to a high level of 6×10^{19} cm^{-3}. Then, $N_{\rm tp} = 6 \times 10^{19}$ cm^{-3} appears to be a turning point of cell performance, in accordance with the variations of η and FF [see Fig. 2(a) and (d)], at which the considerable trapping effect begins to emerge. The drop of V_D associates with the weakening of the built-in field, which directly accounts to the sharp fall of $V_{\rm OC}$ in Fig. 2(b). We also examine the impact of V_D on $J_{\rm SC}$ by demonstrating free hole density in Fig. 3(b). Because the decreased V_D brings about an unfavorable potential barrier to block the collection of holes flowing from the n-type c-Si to the front contact, a large density of holes accumulate, which can hardly be extracted, leading to a drastic deterioration of $J_{\rm SC}$, as shown in Fig. 2(c), and in FF, as shown in Fig. 2(d).

We then turn to the investigation of the shift of SCR from the c-Si to a-Si:H side. The shift of SCR boundary of the c-Si side can be identified from the hole recombination rate R_p plotted in Fig. 5(a) (open circuit). The peak of R_p in the c-Si region corresponds to the position in SCR where most of the defects (i.e., the Gaussian peaks) lie between the two quasi-Fermi level, causing most recombination to happen. Thus, we can see the shift of SCR boundary through the movement of the R_p peak and clearly find that the SCR width of the c-Si side shrinks with the increment of $N_{\rm tp}$. At low $N_{\rm tp}$ of $1 \times 10^{18}-1 \times 10^{19}$ cm^{-3}, the peaks of R_p are not obvious for the high recombination in the c-Si region (position $> 10^{-5}$ cm). However, when $N_{\rm tp}$ increases to the extreme high, i.e., 7×10^{19} cm^{-3}, the near absence of SCR in the c-Si side indicates that the electric field is localized at the a-Si:H/c-Si interface and penetrates little into the bulk of c-Si. This condition causes holes to accumulate over the whole c-Si region [see Fig. 3(b)], accounting for the sharp fall of FF and η, as shown in Fig. 2(a) and (d).

Furthermore, we note that, in Fig. 5(a), R_p abnormally decreases near the front contact ($\sim$1 nm) at very high $N_{\rm tp} > 6 \times 10^{19}$ cm^{-3}. This case can be explained by the increased recombination centers due to the high DOS in the emitter layer. Based on the free-electron density shown in Fig. 5(b), we see that nearly all the electrons from the n-type layer are recombined through recombination centers as soon as they diffuse into the p-type a-Si:H layer. As a result, few electrons can reach the contact to recombine with the holes, which will be collected at the front contact. This condition may also account for the observed abnormal increase of $J_{\rm SC}$ in Fig. 2(c).

Similarly, through the analysis of V_D and SCR width, we can obtain a series of turning points of the cell performance under different doping concentrations $(N_A = 3 \times 10^{19}-3 \times 10^{20}$ cm$^{-3})$, as listed in Table II (symmetry DOS distribution). The DOS distributions also change with N_A according to our model in Section III. The turning point indicates an $N_{\rm tp}$ value at which considerable trapping effect begins to emerge, resulting in an overall decline of cell output and a substantial drop of efficiency to about 15%. It is observed that $N_{\rm tp}$ is close to the value of N_A at relatively low $N_A < 1 \times 10^{20}$ cm^{-3}, whereas with N_A exceeding to a high level of 2×10^{20} cm^{-3}, $N_{\rm tp}$ only slightly increases to 8×10^{19} cm^{-3}, much lower than N_A, which is difficult to realize in practical processes, particularly in such an ultrathin a-Si:H film (6.5 nm) [2], [14]. As a result, the trapping effect turns out to be a serious problem and is difficult to avoid in case of high N_A, and the cell output may further decline if the deterioration of optical properties in heavily doping films is included. This conclusion matches well with the simulations under low N_A [9] but is in contrast to the argument that high N_A of 2×10^{20} cm^{-3} is optimized to achieve the highest efficiency [8], simply benefiting from our improved elaborate DOS model, including the change of the distribution of defect density.

Moreover, because the broken symmetry distribution of DB states $(N_{\rm tA} \neq N_{\rm tD})$ caused by various kinds of defects is very common and widely described by many authors [18], we should also examine the influence of the asymmetry condition to study the realistic effect in practical processes. Table II illustrates the turning points of N_t for both symmetry and asymmetry distributions with increasing N_A The asymmetry DOS distribution is assumed to be $N_{\rm tA} : N_{\rm tD} = 1:5$ (then, $N_{\rm tp} = N_{\rm tD}$), i.e., the neutral DB states D^0 account for a dominate part in the p-type layer. Compared to the values for symmetry distribution of defect states, the difference between corresponding turning points becomes larger with the increment of N_A. Consequently, the introduced defect states asymmetry may aggravate the unfavorable trapping effect, particularly in case of high N_A. This condition underlines the crucial role of good passivation of the emitter layer to suppress the trapping effect under high doping concentrations to achieve high cell efficiency above 20%.

Based on Table II and Fig. 3, we can also find that the Fermi energy level shifts away from the valence band edge as $N_{\rm tp}$ increases. When the effective doping level $E_F - E_V$ (the distance of the Fermi energy level to the valence band edge) reaches 150–190 meV, which is a common value for doped a-Si:H films, the cell performance suffers from the severe trapping effect and drastically deteriorates. This condition also

TABLE II
CALCULATED TURNING POINTS UNDER A SERIES OF DOPING CONCENTRATIONS (N_A) FOR BOTH SYMMETRY AND ASYMMETRY DISTRIBUTION OF DEFECT STATES IN THE P-TYPE EMITTER LAYER, WHERE THE ASYMMETRY DOS DISTRIBUTION IS ASSUMED AS $N_{\mathrm{tA}} : N_{\mathrm{tD}} = 1 : 5$ (THEN, $N_{\mathrm{tp}} = N_{\mathrm{tD}}$). THE CORRESPONDING EFFECTIVE DOPING LEVEL, I.E., THE DIFFERENCE OF THE FERMI LEVEL TO THE VALENCE BAND EDGE $E_F - E_V$, AT THE TURNING POINT IS ALSO DEMONSTRATED

N_A (cm^{-3})	Symmetry DOS distribution		Asymmetry DOS distribution	
	Turning point (cm^{-3})	E_F-E_V (eV)	Turning point (cm^{-3})	E_F-E_V (eV)
3.0×10^{19}	1.5×10^{19}	0.16	1.4×10^{19}	0.15
7.5×10^{19}	6.0×10^{19}	0.15	5.5×10^{19}	0.14
1.0×10^{20}	7.0×10^{19}	0.14	6.4×10^{19}	0.14
2.0×10^{20}	8.2×10^{19}	0.15	7.5×10^{19}	0.15
3.0×10^{20}	9.5×10^{19}	0.14	8.5×10^{19}	0.14

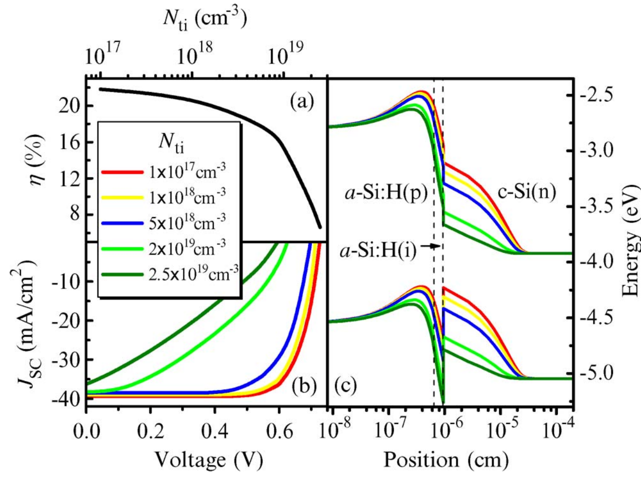

Fig. 6. Effect of the density of DB states (N_{ti}) in the intrinsic a-Si:H buffer layer on the HIT cell of (a) conversion efficiency (η), (b)–V curves, and (c) band diagram under illumination under the open-circuit condition.

raises the importance of controlling the activation energy of a-Si:H films used for HIT solar cells, particularly under heavy doping conditions.

V. EFFECT OF INCREASING THE AMOUNT OF DEFECTS IN INTRINSIC BUFFER LAYERS

Although the DOS in the intrinsic a-Si:H layer is usually lower than in doped layers [14], [16], [17], it can also become pronounced to worsen the cell performance, particularly when the emitter layer is considerably defective. Fig. 6(a) and (b) illustrates the dependence of the density of DB states (N_{ti}) in the intrinsic a-Si:H buffer layer on HIT cell performance under conditions of the highly defective emitter layer with $N_{\mathrm{tp}} = 4 \times 10^{19}$ cm^{-3} (where N_A retains 7.5×10^{19} cm^{-3}). We vary N_{ti} in the range of 1.0×10^{17} cm^{-3}2.5×10^{19} cm^{-3} and clearly show that all aspects of the HIT cell performance, including V_{OC}, J_{SC}, FF, and η, rapidly fall when N_{ti} rises to higher than 5×10^{18} cm^{-3}. This result matches well with the study of Rahmouni *et al.* [5] on the passivation of the intrinsic buffer layer, and thus, we can further devote to the mechanism of trapping effect in the intrinsic buffer layer based on our improved DOS model.

We plot the band diagram under illumination (open-circuit) in Fig. 6(c) to figure out how N_{ti} affects the cell output. Both V_D and the depletion region width are observed to significantly drop as N_{ti} ascends beyond 5×10^{18} cm^{-3}, and for even higher $N_{\mathrm{ti}} > 2 \times 10^{19}$ cm^{-3}, the depletion region nearly vanishes. These behaviors indicate the decrease of the built-in field and a shrink of the SCR, causing a pronounced trapping effect. We also introduce the charge trapped in defect states in the intrinsic layer (Q_{ti}) to understand the impact of N_{ti} on the built-in field and SCR. Through (5) and the DOS distribution model established in Section III, we find that Q_{ti} is positive and increases with N_{ti}. Then, the charge neutrality condition in the SCR should be modified as

$$-L_p N_A + \sum Q_{\mathrm{tp}} + \sum Q_{\mathrm{ti}} + L_n N_D = 0 \qquad (6)$$

where L_p and L_n are the SCR widths of the p-type a-Si:H side and the n-type c-Si side, respectively. ΣQ_{tp} and ΣQ_{ti} stand for the total charge trapped in defect states over the whole p-type and intrinsic a-Si:H layers, respectively. Here, free electrons and holes can be neglected under high N_A, as well as the case of charge trapped in c-Si for its low DOS (see Table I).

The positive Q_{ti} can be recognized as an n-type background doping in the intrinsic a-Si:H layer. When Q_{ti} exceeds beyond N_D, the background doping can substantially reduce the difference of effective doping concentration between the p- and n-type layers, leading to the decrease of built-in field and the shrink of SCR, as discussed in Section IV, which account for the decline of the HIT cell performance. At the high level of $N_{\mathrm{ti}} > 5 \times 10^{18}$ cm^{-3}, Q_{ti} sufficiently increases to reduce the space charge, resulting in the rearrangement of bands to keep charge balance. Moreover, N_{ti} should exhibit a much more negative effect on HIT cell performance if the multistep tunneling of electrons from the conduction band of c-Si through the localized states in the intrinsic layer to the p-type a-Si:H layer is

included in our simulation. Other researchers have considered the multistep tunneling progress as an undesirable channel for electrons to recombine with holes at the front contact and get an overall decline of all aspects of the cell performance [5]. In other words, in practical processes, the DOS in the intrinsic buffer a-Si:H layer should further be suppressed, at least to the level of $N_{\mathrm{ti}} < 5 \times 10^{18}$ cm^{-3}, to obtain satisfactory HIT cell performance.

VI. Conclusion

We have employed the numerical simulator AFORS-HET to model HIT solar cells with Sanyo's structure of TCO/p-a-Si:H/i-a-Si:H/n-c-Si/n$^+$-a-Si:H/AlBSF, paying special attention to the effect of the DOS in both the p-type a-Si:H emitter and the intrinsic a-Si:H buffer layers. We have established a detailed DOS distribution in a-Si:H layers, including both bandtail states and deep DB states, through the experimental results yielded from various measurements by former researchers. The DOS distribution model has been employed to calculate the charge trapped in defect states to understand the drop of the built-in field and shift of the SCR from the c-Si to the a-Si side with the increase of DOS, which result in an observed sharp fall of all aspects of HIT cell performance. We find that the DOS in the p-type a-Si:H emitter layer can cause a considerable trapping effect, resulting in a decline of cell performance that is difficult to avoid, particularly under high doping concentration beyond 1×10^{20} cm^{-3}, whereas the DOS in the intrinsic a-Si:H buffer layer brings about an unfavorable background doping due to the increment of charge trapped in defect states, leading to a substantial cut of the cell output at a density of DB states of 5×10^{18} cm^{-3}. In this paper, we have suggested proper DOS in the p-type emitter a-Si:H layer required for high efficiency of HIT cells above 20% under different doping concentrations, whereas the DOS in the intrinsic buffer layer should be suppressed to below 5×10^{18} cm^{-3}. Further work is currently on the way for the study of the DOS effect in HIT solar cells with graded heterojunction, instead of the abrupt heterojunction here, which can more accurately describe the band bending and band offsets in HIT structures.

References

[1] T. Mishima, M. Taguchi, H. Sakata, and E. Maruyama, "Development status of high-efficiency HIT solar cell," *Solar Energy Mater. Solar Cells*, vol. 95, no. 1, pp. 18–21, Jan. 2011.

[2] M. Schmidt, L. Korte, A. Laades, R. Stangl, C. Schubert, H. Angermann, E. Conrad, and K. v. Maydell, "Physical aspects of a-Si:H/c-Si heterojunction solar cells," *Thin Solid Films*, vol. 515, no. 19, pp. 7475–7480, Jul. 2007.

[3] M. R. Page, E. Iwaniczko, Y.-Q. Xu, L. Roybal, F. Hasoon, Q. Wang, and R. S. Crandall, "Amorphous/crystalline silicon heterojunction solar cells with varying i-layer thickness," *Thin Solid Films*, vol. 519, no. 14, pp. 4527–4530, May 2011.

[4] M. Tucci and G. de Cesare, "17% efficiency heterojunction solar cell based on p-type crystalline silicon," *J. Non-Cryst. Solids*, vol. 338–340, pp. 663–667, Jun. 2004.

[5] M. Rahmouni, A. Datta, P. Chatterjee, J. Damon-Lacoste, C. Ballif, and P. Roca i Cabarrocas, "Carrier transport and sensitivity issues in heterojunction with intrinsic thin-layer solar cells in n-type crystalline silicon: A computer simulation study," *J. Appl. Phys.*, vol. 107, no. 5, pp. 054 521-1–054 521-14, Mar. 2010.

[6] A. Kanevce and W. K. Metzger, "The role of amorphous silicon and tunneling in heterojunction with intrinsic thin-layer (HIT) solar cells," *J. Appl. Phys.*, vol. 105, no. 9, pp. 094 507-1–094 507-7, Mar. 2009.

[7] M. Taguchi, E. Maruyama, and M. Tanaka, "Temperature dependence of amorphous/crystalline silicon heterojunction solar cells," *Jpn. J. Appl. Phys.*, vol. 47, no. 2, pp. 814–818, Feb. 2008.

[8] L. Zhao, C. L. Zhou, H. L. Li, H. W. Diao, and W. J. Wang, "Design optimization of bifacial HIT solar cells on p-type silicon substrates by simulation," *Solar Energy Mater. Solar Cells*, vol. 92, no. 6, pp. 673–681, Jun. 2008.

[9] N. Hernández-Como and A. Morales-Acevedo, "Simulation of heterojunction silicon solar cells with AMPS-1D," *Solar Energy Mater. Solar Cells*, vol. 94, no. 1, pp. 62–67, Jan. 2010.

[10] L. Korte, E. Conrad, H. Angermann, R. Stangl, and M. Schmidt, "Advances in a-Si:H/ c-Si heterojunction solar cell fabrication and characterization," *Solar Energy Mater. Solar Cells*, vol. 93, no. 6/7, pp. 905–910, Jun. 2009.

[11] A. Datta, J. Damon-Lacoste, P. Roca i Cabarrocas, and P. Chatterjee, "Defect states on the surface of a p-type c-Si wafer and how they control the performance of a double heterojunction solar cell," *Solar Energy Mater. Solar Cells*, vol. 92, no. 11, pp. 1500–1507, Nov. 2008.

[12] A. Froitzheim, K. Brendel, L. Elstner, W. Fuhs, K. Kliefoth, and M. Schmidt, "Interface recombination in heterojunctions of amorphous and crystalline silicon," *J. Non-Cryst. Solids*, vol. 299–302, pp. 663–667, Apr. 2002.

[13] A. Datta, M. Rahmouni, M. Nath, R. Boubekri, P. Roca i Cabarrocas, and P. Chatterjee, "Insights gained from computer modeling of heterojunction with intrinsic thin-layer (HIT) solar cells," *Solar Energy Mater. Solar Cells*, vol. 94, no. 9, pp. 1457–1462, Sep. 2010.

[14] M. Schmidt, A. Schoepke, L. Korte, O. Milch, and W. Fuhs, "Density distribution of gap states in extremely thin a-Si:H layers on crystalline silicon wafers," *J. Non-Cryst. Solids*, vol. 338–340, pp. 211–214, Jun. 2004.

[15] L. Korte, A. Laades, and M. Schmidt, "Electronic states in a-Si:H/c-Si heterostructrues," *J. Non-Cryst. Solids*, vol. 352, no. 9–20, pp. 1217–1220, Jun. 2006.

[16] K. Winer, I. Hirabayashi, and L. Ley, "Distribution of occupied near-surface band-gap states in a-Si:H," *Phys. Rev. B*, vol. 38, no. 11, pp. 7680–7693, Oct. 1988.

[17] M. Stutzmann, D. K. Biegelsen, and R. A. Street, "Detailed investigation of doping in hydrogenated amorphous silicon and germanium," *Phys. Rev. B*, vol. 35, no. 11, pp. 5666–5701, Apr. 1987.

[18] M. Mikolášek, J. Racko, L. Harmatha, P. Gašpierik, and P. Šutta, "Influence of the broken symmetry of defect state distribution at the a-Si:H/c-Si interface on the performance of heterojunction solar cells," *Appl. Surf. Sci.*, vol. 256, no. 18, pp. 5662–5666, Jul. 2010.

[19] W. Shockley and W. T. Read, "Statistics of the recombinations of holes and electrons," *Phys. Rev.*, vol. 87, no. 5, pp. 835–842, Sep. 1952.

[20] J. M. Essick and J. D. Cohen, "Band offsets and deep defect distribution in hydrogenated amorphous silicon–crystalline silicon heterostructure," *Appl. Phys. Lett.*, vol. 55, no. 12, pp. 1232–1234, Sep. 1989.

[21] H. Mimura and Y. Hatanaka, "Energy band discontinuities in a heterojunction of amorphous hydrogenated Si and crystalline Si measured by internal photoemission," *Appl. Phys. Lett.*, vol. 50, no. 6, pp. 326–328, Feb. 1987.

[22] J. Schmidt, "Light-induced degradation in crystalline silicon solar cells," *Solid State Phenom*, vol. 95/96, pp. 187–196, 2004.

[23] W. B. Jackson, S.-J. Oh, C. C. Tsai, and J. W. Allen, "Conduction-band density of states in hydrogenated amorphous silicon determined by inverse photoemission," *Phys. Rev. Lett.*, vol. 53, no. 15, pp. 1481–1484, Oct. 1984.

[24] I. Hirabayashi, K. Winer, and L. Ley, "Photomodulation of the photoelectric yield from a-Si:H," *J. Non-Cryst. Solids*, vol. 97/98, pp. 87–90, Dec. 1987.

[25] D. V. Lang, J. D. Cohen, and J. P. Harbison, "Measurement of the density of gap states in hydrogenated amorphous silicon by space charge spectroscopy," *Phys. Rev. B*, vol. 25, no. 8, pp. 5285–5320, Apr. 1982.

[26] J.-K. Lee and E. A. Schiff, "Modulated electron-spin-resonance measurements and defect correlation energies in amorphous silicon," *Phys. Rev. Lett.*, vol. 68, no. 19, pp. 2972–2975, May 1992.

[27] J. D. Cohen, J. P. Harbison, and K. W. Wecht, "Identification of the dangling-bond state within the mobility gap of a-Si:H by depletion-width-modulated ESR spectroscopy," *Phys. Rev. Lett.*, vol. 48, no. 2, pp. 109–112, Jan. 1982.

[28] Z. Vardeny, T. X. Zhou, H. A. Stoddart, and J. Tauc, "Photomodulation spectroscopy of dangling bonds in doped and undoped a-Si:H," *Solid State Commun.*, vol. 65, no. 9, pp. 1049–1053, Mar. 1988.

X. Hua was born in Wuxi, China, on June 11, 1989. He received the B.S. degree in physics from Shanghai Jiao Tong University, Shanghai, China, in 2009. Since 2009, he has been a Ph.D. candidate in the Department of Physics, Shanghai Jiao Tong University.

His research interests include semiconductor device physics and solar cells.

Z. P. Li was born in Gaoan, China, on December 27, 1975. He received the Ph.D. degree in materials science and engineering from the Chinese Academy of Sciences, China, in 2003.

From 2009 to 2011, he was a Postdoctoral Research Fellow with the Department of Physics, Shanghai Jiao Tong University, Shanghai, China, where he is currently an Assistant Professor with the Institute of Solar Energy. His research interests include solar energy materials and solar cells.

W. Z. Shen was born in Suzhou, China, on May 22, 1968. He received the Ph.D. degree in semiconductor physics and semiconductor device from the Chinese Academy of Sciences, China, in 1995.

From 1995 to 1996, he was an Assistant Professor with the National Laboratory for Infrared Physics, Shanghai Institute of Technical Physics, Chinese Academy of Sciences. From 1996 to 1999, he was a Research Associate with the Department of Physics and Astronomy, Georgia State University, Atlanta. Since 1999, he has been a Full Professor with the Department of Physics, Shanghai Jiao Tong University, Shanghai, China, where he is currently the Director of the Institute of Solar Energy, leads the Laboratory of Condensed Matter Spectroscopy and Optoelectronic Physics, and has been the Director of the Key Laboratory of Artificial Structures and Quantum Control (Ministry of Education) since 2009. From 2000 to 2005, he was the Changjiang Chair Professor with the National Ministry of Education, Shanghai Jiao Tong University. From 2005 to 2008, he led the Changjiang Innovation Group, National Ministry of Education. He is the author and or a coauthor of more than 200 papers and three book chapters. He is the holder of 18 granted patents. His research interests include optical and electrical properties of semiconductors, as well as semiconductor quantum electronic devices and solar cells.

Dr. Shen is the Chair of the Shanghai Solar Energy Society. He received the 2001 Chinese Distinguished Young Scientist Award.

G. Y. Xiong was born in Shanghai, China, on July 2, 1978. He received the Ph.D. degree from Boston College, Chestnut Hill, MA, in 2007.

From 2007 to 2008, he was with Boston College as a Postdoctoral Researcher. In 2009, he joined a project that focuses on environmental improvement at Shanghai. Since 2010, he has been a Senior R&D Engineer with the R&D Center, Canadian Solar Inc., Suzhou, China. His research interests include high-efficiency solar cells and nanotechnology applications.

X. S. Wang was born in Suzhou, China, on January 23, 1977. He received the Ph.D. degree in mechanical engineering from the Hong Kong University of Science and Technology, Kowloon, Hong Kong, in 2006.

From 2006 to 2008, he was with the R&D Center, Solarfun, as the Vice Director. Since 2008, he has been the Technical Director with the R&D Center, Canadian Solar Inc. His research interests include solar wafers, cells, and modules.

L. J. Zhang was born in Huangyan, China on December 13, 1966. He received the Ph.D. degree in semiconductor physics and semiconductor devices from the Chinese Academy of Sciences, Beijing, China, in 1992.

From 1993 to 1996, he was a Project Manager with the China Hi-Tech Group Company. From 1997 to 1999, he was a Production Manager with Shanghai Temic Telefunken Semiconductor Company. From 1999 to 2003, he was a Production Manager/Operations Manager with Shanghai Simconix Electronic Company Ltd. In June 2003, he was with the Canadian Solar Inc. as the Deputy General Manager and the Technical Director. He is currently the General Manager and the Vice President of Technology and Business Expansion with CSI Cells Ltd. Company. His research interests include solar wafers, cells, and modules.